

# Power Flow Control of PV-Wind-Battery Hybrid Renewable Energy Systems for Stand-Alone Application

Somnath Das\*<sup>‡</sup>, A. K. Akella\*

\*Department of Electrical Engineering, National Institute of Technology, Jamshedpur, India-831014

(somnathdasju@gmail.com, akakella@nitjsr.ac.in)

<sup>‡</sup>

Corresponding Author: Somnath Das, Department of Electrical Engineering, National Institute of Technology, Jamshedpur, India-831014, somnathdasju@gmail.com

*Received: 18.05.2017 Accepted:25.07.2017*

**Abstract-** The main problem in renewable energy system is the variation in power generation from time to time due to the intermittent nature of the renewable sources. Miss matching between power generation and load power causes a deviation from the desired voltage and frequency in power supply. A power flow control of photovoltaic-wind-battery Hybrid Renewable Energy System (HRES) for stand-alone application is presented here to balance the power generation and load power. A control strategy is implemented with fuzzy logic controller for smoothing of the power fluctuation and at the same time to maintain the battery state of charge (SOC) within allowable limits. The various components are modeled and simulated in MATLAB/Simulink. Simulation study is done at changing nature of power generation and load demand with an initial battery SOC. The results obtained show that in spite of sudden load changes and changes in the power generation, the power balance between the supply and demand effectively maintained by the proposed fuzzy logic based controller (FLC). The power fluctuation is suppressed and supply a good quality power while maintaining SOC within limits.

**Keywords-** Power control; Hybrid Renewable Energy Systems; Battery charge/discharge control.

## 1. Introduction

Due to the rapid depletion of fossil fuel and environment pollution people are now attracted towards non conventional energy sources like PV, wind, hydro etc. Solar and wind energy resources are abundantly available all over the world. For the fluctuating nature of renewable energy resources power generation from renewable energy systems are intermittent. These circumstances motivated to combine two or more energy sources with storage system to make Hybrid Renewable Energy System [1–3]. An isolated hybrid system gives a higher efficiency with a low cost of energy production, compared to the system with a single source [4]. It is necessary to take care of changes in the generated power which is varying from time to time [5]. In literature [5-10] different types of HRES are introduced which are working in grid connected or stand-alone mode. HRES system energy management is done by using PI controller in [6, 9]. It is done by controlling a buck-boost bidirectional converter for battery charging and discharging. A current control strategy for power balance is presented by PI controller in [8]. The conventional controller design depends on mathematical modeling of the system. For complex system the mathematical model cannot be properly defined. In spite of

all the system parameters are known, there may be parameter variations during the operation of the system. So it is difficult to design controller parameters and more time is required [10]. Many researchers are worked with latest controllers such as predictive controller [11], sliding mode controller [12], H-infinity controller [13] for better steady state and transient response of systems. These control techniques depend on complex mathematical analysis. In order to avoid the difficulties in controller designing, intelligent controllers are used [14]. For better results intelligent controller are now applied in various hybrid energy system problems [15-17]. An application of FLC for inverter voltage and frequency control is shown in [10]. FLC works very well even after variations in system parameter and operating conditions [17]. Here a fuzzy logic based controller for battery charging or discharging is proposed and implemented for system power flow control to suppress the power fluctuation and to supply a quality power to load.

## 2. Configuration and Modeling of the HRES

The HRES shown in “fig.1” comprises of PV system, permanent magnet synchronous generator (PMSG) based

the cell in °k and  $q(=1602 \cdot 10^{-19} \text{ C})$  is the electron charge. Photocurrent is given by following equation (2),

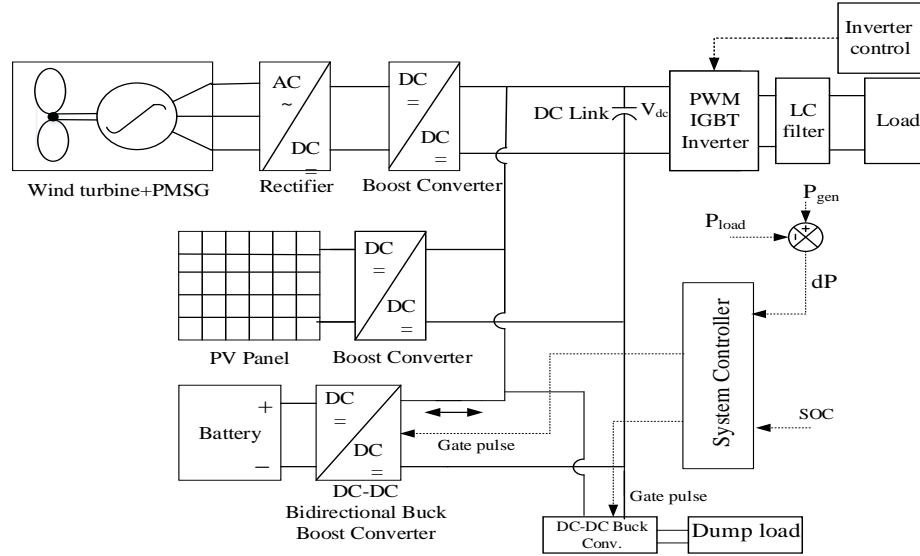


Fig.1. HRES for the proposed controller implementation

wind systems and battery storage. The PV and wind systems having its own DC-DC boost converter equipped with MPPT controller. In this work, very well known Perturb and Observe (P&O) MPPT technique is adopted [18] for maximum power extraction. The battery system has its bidirectional buck-boost converter. The battery is charged or discharged depending on the availability of excess or shortage of power. A fuzzy logic based controller is designed for the charge and discharge of the battery. The DC link capacitor is connected to the sinusoidal PWM IGBT based inverter which is fed to single phase AC load. The harmonics present in the output of the Inverter is filtered by a LC filter. The maximum power ratings of PV and wind systems considered here are 6kW and 4 kW respectively and battery rating taken here 6 kWh.

### 2.1. PV System Modeling

A solar cell converts photon energy into electrical energy. Single diode solar cell model is used here. The current generated from the PV cell is represented by following equation (1) [9],

$$I = I_{ph} - I_s \left[ \exp \frac{q(V + IR_s)}{NKT} - 1 \right] - \frac{V + IR_s}{R_{sh}} \quad (1)$$

Here,  $I$  and  $V$  are the harvested current and voltage,  $I_{ph}$  is the photocurrent,  $I_s$  is the diode reverse saturation current,  $N$  ( $=2$ ) denotes the ideality factor of the diode,  $R_s$  and  $R_{sh}$  is the series and parallel resistance respectively,  $K$  ( $=1380.10^{-23} \text{ j/k}$ ) known as Boltzmann constant,  $T$  is the temperature of

$$I_{ph} = [I_{sc} + K_i(T - 298)] \frac{G}{1000} \quad (2)$$

Here,  $I_{sc}$  is the photocurrent at  $T=25^\circ\text{C}$  and  $G=1000 \text{ W/m}^2$   $G$  is irradiance,  $K_i$  ( $=0.0032$ ) is the short circuit current temperature coefficient. Diode reverse saturation current is given by equation (3),

$$I_s = I_{rs} \left( \frac{T_c}{T_{ref}} \right)^3 \exp \left[ \left( \frac{I}{T_{ref}} - \frac{1}{T_c} \right) \frac{E_g}{N V_t} \right] \quad (3)$$

Here  $I_{rs}$  is the reverse saturation current at  $25^\circ\text{C}$ ,  $V_t$  indicates thermal voltage,  $E_g$  denotes the band gap energy,  $T_c$  denotes cell working temperature,  $T_{ref}$  denotes reference cell temperature ( $25^\circ\text{C}$ ).

### 2.2. Wind System Modeling

The PMSG model is described in a d-q quadrature rotor-fixed reference by equation given in equations (4), (5) and (6) [19, 20]

$$\frac{di_q}{dt} = -\frac{R_s}{L_s} i_q - \omega_e i_d + \frac{\omega_e \phi_e}{L_s} - \frac{\pi V_{red} i_q}{3\sqrt{3} L_s \sqrt{i_q^2 + i_d^2}} D_\omega \quad (4)$$

$$\frac{di_d}{dt} = -\frac{R_s}{L_s} i_d + \omega_e i_q - \frac{\pi V_{red} i_d}{3\sqrt{3} L_s \sqrt{i_q^2 + i_d^2}} D_\omega \quad (5)$$

$$\frac{d\omega_e}{dt} = \frac{P}{2J} \left( T_t - \frac{3P}{4} \phi_e i_q \right) \quad (6)$$

Where  $i_d$  and  $i_q$  are the direct and quadrature currents respectively.  $\omega_e$ ,  $R_s$  and  $L_s$  indicates the angular speed, stator phase resistance and inductance, respectively.  $P$ ,  $J$ ,  $\phi_e$  and  $V_{red}$  indicates the pole number of the generator, the inertia of the rotating parts, the flux linkages and the rectifier voltage, respectively.  $D_\omega$  denotes duty cycle of the boost converter; wind turbine torque is defined by  $T_t$  which is shown in equation (7)

$$T_t = \frac{P_t}{\omega_m} = \frac{1}{2\omega_m} C_p \cdot \rho \cdot A \cdot v_w^3 \quad (7)$$

Here  $P_t$  is the power of turbine,  $\omega_m$  is the mechanical speed of the PMSG,  $C_p$  is the power coefficient,  $\rho$  is the air density,  $A$  is the turbine swept area, and  $V$  is the wind speed.

### 2.3. The Storage System Modeling

In this work, a Lead acid battery model is considered as controlled voltage source which is connected in series with a fixed resistance [21]. The battery voltage ( $V_{batt}$ ) is given by equation (8)

$$V_{batt} = E - R_{batt} I_{batt} \quad (8)$$

$I_{batt}$ ,  $R_{batt}$  and  $E$  are the battery current, internal resistance and voltage.

$$E = E_o - K \frac{Q}{Q - \int Idt} + A \exp(-B \int Idt) \quad (9)$$

Here,  $E_o$ ,  $K$  and  $Q$  are the battery constant voltage, the polarization voltage and the battery capacity.  $\int Idt$  defines the actual battery charge by taking  $I$  as current.  $A$  is the exponential zone amplitude and  $B$  is the exponential zone time constant inverse. The SOC of the battery is presented in equation (10)

$$SOC(t) = 100 \left( 1 - \frac{\int Idt}{Q} \right) \quad (10)$$

To increase battery life, state of charge of a battery must be maintained within allowable limits. The SOC minimum and maximum limits of the Lead-acid battery are taken at 20 and 80% [22].

### 2.4. Dump Load Model

It is presented as a constant resistor whose voltage is varying over time. It is linked with DC link capacitor through a DC/DC buck converter. The dump load consumes power when there is excess power and there by balancing power generation and consumption. The buck converter switching depends on the available excess power  $P_{dump}$ . The duty ratio ( $d$ ) for the buck converter is calculated as in equation (11)

$$d = \frac{V_0}{V_{dc}} = \sqrt{\frac{R_{dump} P_{dump}}{V_{dc}^2}} \quad (11)$$

Here the voltage across the dump load is  $V_0$ ,  $R_{dump}$  is the resistance of dump load.

### 2.5. Model of the DC-AC Converter with Voltage and Frequency Control

It is required to supply the load with certain voltage and frequency and it is done by the inverter control. Here first the voltage at load is sensed ( $V_m$ ) and compare with the desired reference value ( $V_{ref}$ ) and the difference between them is given to proportional plus integral (PI) controller [23]. A sine wave having amplitude 1 and frequency 50 Hz is multiplied to generate the reference signal. This reference signal produces the PWM pulses to switch on/off the voltage source inverter. The diagram of the control scheme is given in "Fig.2". LC filter is connected after PWM inverter in order to eliminate the high frequency harmonics from output AC voltage. The LC filter design is undertaken as it is given in [24].

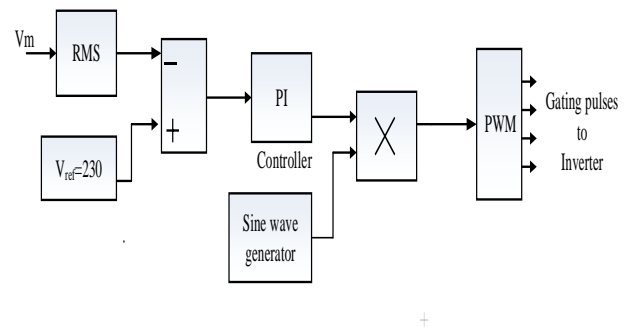


**Fig.2.** PWM inverter controller for load voltage and frequency control

### 3. Fuzzy Logic Based Controller Design

The flowchart of power flow control strategy of the HRES is shown in "fig.3". The system operates in 4 modes. For all the modes total power generation  $P_{gen}$  (PV plus wind power) is measured first then it compares with load demand  $P_{load}$ ,  $dP (=P_{gen}-P_{load})$  and SOC are measured. Different modes of operation are given below,

Mode-1: In this mode  $P_{gen}$  is greater than  $P_{load}$  and SOC is less than 0.8, battery will be charged. In this mode the buck mode of the buck-boost converter will be in operation according to the controller battery reference power  $P_{batref}$ . So the power balance equation is

$$P_{gen} - P_{bat} = P_{load} \quad (12)$$

Mode-2:  $P_{gen}$  is more than  $P_{load}$  and SOC is more than 0.8, battery will not be charged as it touches its maximum limit. In this mode the controller output will be zero so the battery will not be charged or discharged that is it will be in cut off position. So the dump load starts its operation. The power balance equation is

$$P_{gen} - P_{dump} = P_{load} \quad (13)$$

Dump load absorbs the excess power.

Mode-3:  $P_{gen}$  is lower than  $P_{load}$  and SOC is more than 0.2, battery should be discharged to meet the load. In this mode the boost mode of the buck-boost converter will be in operation according to the controller battery reference power  $P_{batref}$ . The power balance equation is

$$P_{gen} + P_{bat} = P_{load} \tag{14}$$

Mode-4:  $P_{gen}$  is lower than  $P_{load}$  and SOC is less than 0.2, so battery will not discharged and system needs to curtail some amount of load to balance the demand and supply.

The controllers implemented are shown in “fig.4” and “fig.5”. The proposed controller for battery charge/discharge control is implemented using FLC. Figure 4 shows the controller for battery charge/discharge. The FLC has three main parts- the fuzzification part receives the inputs to the controller and generates a degree of membership relative to each fuzzy set in the membership function, the inference engine evaluates these fuzzy set memberships and decides which rules should be fired, the defuzzification process receives these values and converts them into an output control signal. Mamdani fuzzy inference method and the centre of mass of the weighted outputs are taken in this work. It has two inputs-  $dP$ , SOC and one output-battery reference power  $P_{batref}$ . Depending on the input values controller generates a desired value for reference battery power. The battery reference power is then divided by the battery voltage to generate the reference current for the battery. PWM signals are generated for the buck-boost converter. The membership functions (MFs) which used for inputs and outputs data are shown in “Figs.6-8” and the rules to be evaluated are given in “Table1.” In “fig.5” dump load converter control is presented. The duty ratio is calculated according to the equation (11).

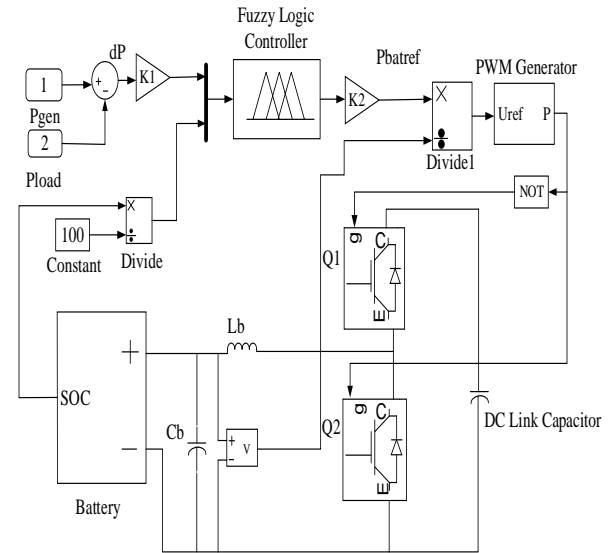


Fig.4. Battery charge/discharge control

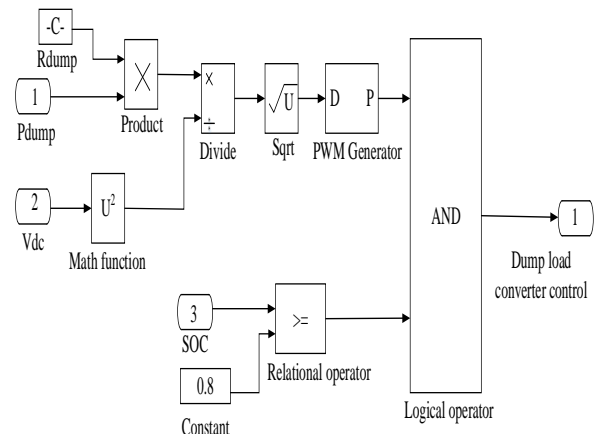


Fig.5. Dump load converter control

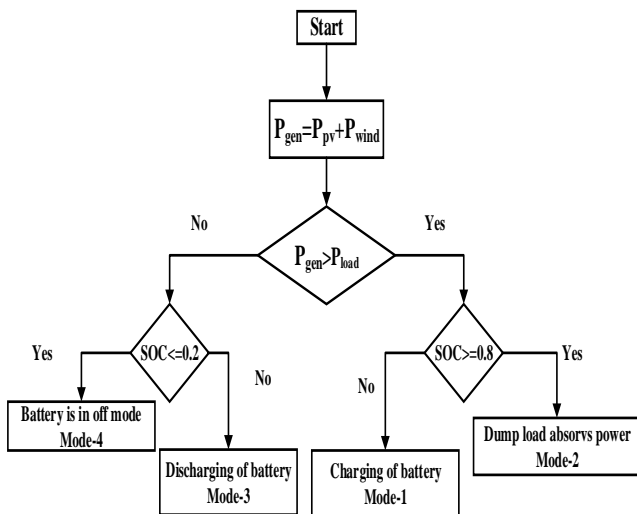


Fig.3. Control strategy for the HRES

Table 1. Fuzzy rules

dP \ SOC	PB	PM	PS	Z	NS	NM	NB
L	NB	NM	NS	Z	Z	Z	Z
M	NB	NM	NS	Z	PS	PM	PB
H	Z	Z	Z	Z	PS	PM	PB

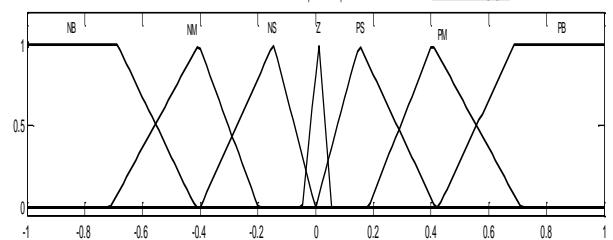


Fig.6. Input dP

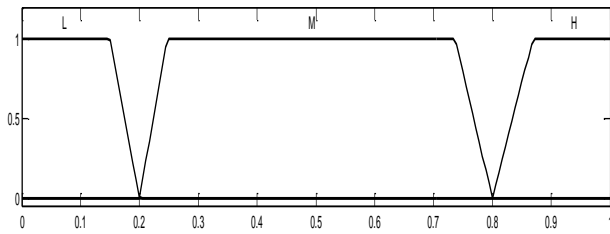


Fig.7. Input SOC

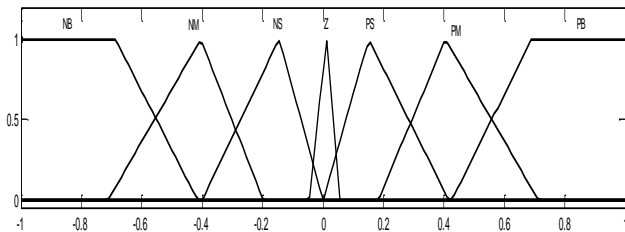


Fig.8. Output  $P_{batref}$

#### 4. Simulation Results and Discussion

The various components of the HRES with the proposed controller are simulated in MATLAB/Simulink. The various parameters for the PV module and wind systems used in simulations are given in “Table 2” and “Table 3”.

Table 2. Parameters of PV module

Parameters	Variable	Value
Maximum power	$P_m$	210 W
Maximum current	$I_m$	7.0A
Maximum voltage	$V_m$	30.0V
Open circuit current	$V_{oc}$	36.5V
Short circuit current	$I_{sc}$	7.8A

Table 3. Parameters of wind system

Parameters	Values
Number of poles (p)	10
Stator resistance ( $R_s$ )	$0.422\Omega$
Magnetic flux linkage	$0.433Wb$
Stator inductance ( $L_s$ )	8.4mH
Moment of inertia (J)	$7.764 kg/m^2$
Rated power	4 kW

Solar irradiance values and wind speed are shown in “fig.9” and “fig.10”. It is varying with time and it shows the randomness in the solar irradiance and wind speed. Battery

SOC in this simulation run is considered 50%. In “fig.9” from time  $t=2$  sec to  $t=3$  sec solar radiation is  $1000 W/m^2$ . The PV power generation is maximum that is 6 kW as seen from “fig.11”. In “fig.10” wind speed is at 12 m/s during time  $t=0$  to  $t=1$ , during this time period wind power is maximum that is 4 kW as seen from “fig.11”. Different powers - PV power, wind power, load power and battery power changing with time(S) as obtained from simulation is shown in “fig.11”.

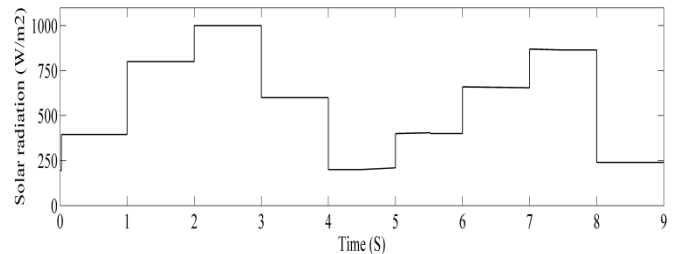


Fig.9. Solar irradiance ( $W/m^2$ )

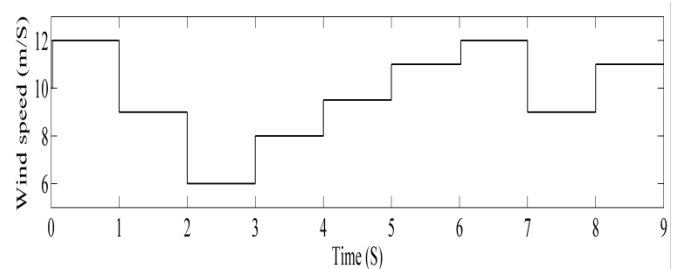


Fig.10. Wind speed (m/s)

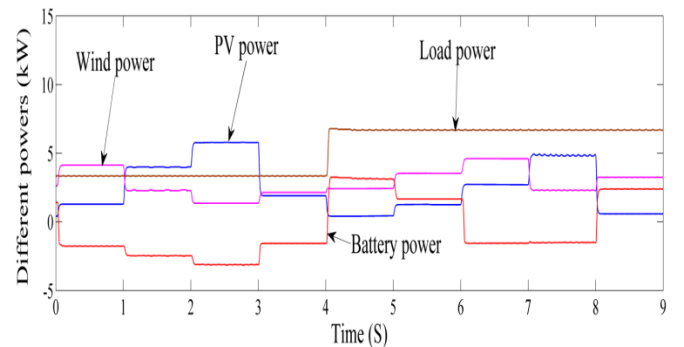


Fig.11. Different power-PV power, wind power, load power & battery power

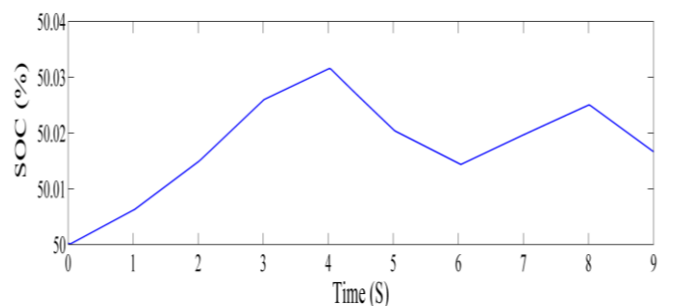
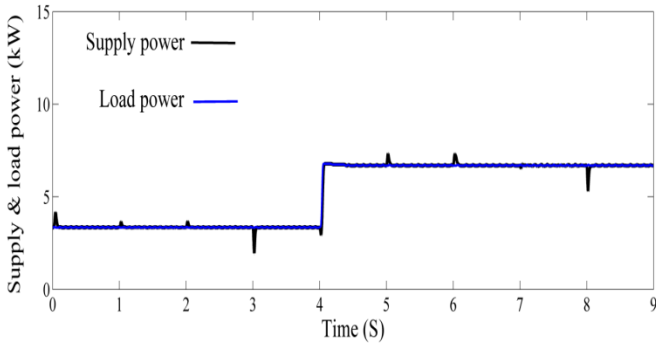


Fig.12. SOC (%)

Load power is initially 3.5 kW and it is changed to 7 kW at time  $t=4$  sec. From time  $t=0$  to time  $t=3$  sec the total power

generation from wind and solar is more than the load power requirement and the battery is charged during this period. From time  $t=3$  to  $t=4$  sec total power generation is equal to power demand that is battery power is 0. From time  $t=4$  sec to  $t=9$  sec total power generation is less than power demand. The battery is discharged during this period to meet the load power. It is seen that the battery power is positive during this time duration. "Figure12" shows the variation in battery SOC. In "fig.13" given below shows the supply and demand power. From the "fig.13" it is seen that total generated power always meet the load power.



**Fig.13.** Total power generation & Load power

In another simulation run battery SOC is considered 81% initially to analyze the dump load operation. It is seen from "fig.14" that from time  $t=0$  to  $t=4$  sec total power generation is more than load demand, battery power is 0 during this time period and dump load is in operation to balance the power. From time  $t=4$  sec to  $t=6$  sec power generation is lower than load demand and battery is discharged to supply the deficit power. During time  $t=6$  to  $t=8$  sec again dump load is in working mode and then the battery discharges again from  $t=8$  to  $t=9$  sec. Battery SOC value as seen from "fig.15" proofs that battery SOC is within limits to protect it from overcharge.

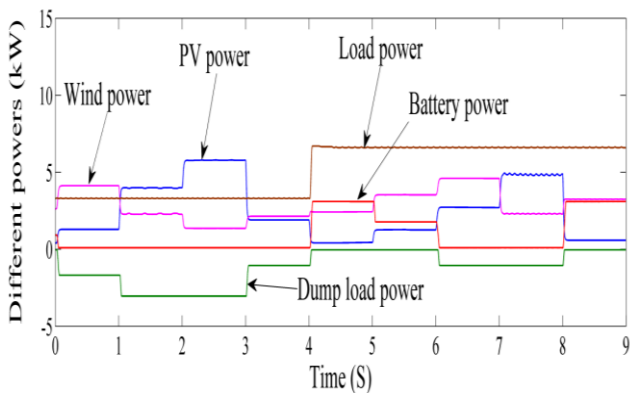


**Fig.14.** Different power-PV power, wind power, load power, battery power & dump load power

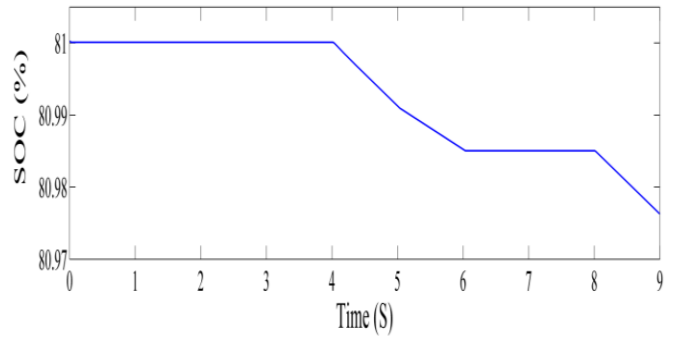


**Fig.15.** Battery SOC (%)

Inverter output voltage and current with LC filter is shown in "fig.16" below and in "fig. 17" the load voltage and current before load changes and after load changes is shown. It is observed from "fig. 17" that load changes at time  $t=4$  sec, the load current increases but load voltage remains fixed and the corresponding rms value is shown in 'fig.18'.

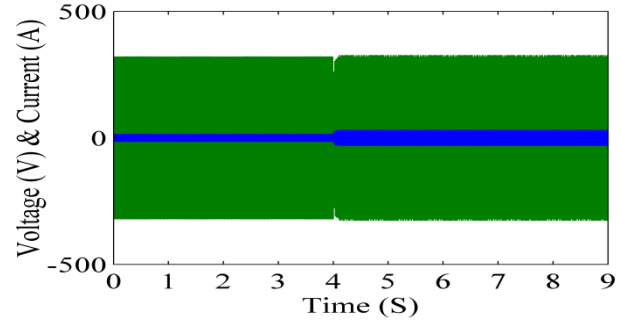


**Fig.16.** Load voltage (V) and current (A)

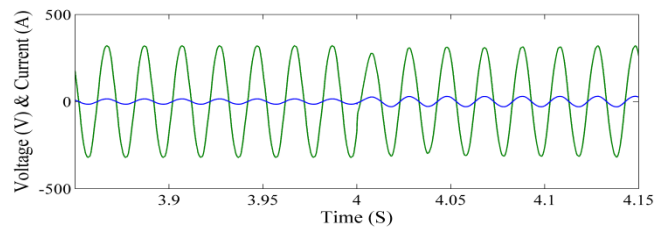


**Fig.17.** Inverter output voltage (V) & current (A) at load change

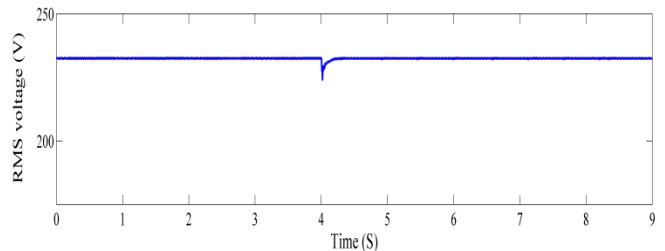


**Fig.18.** RMS value of load voltage (V)

Frequency of load voltage is shown in "fig.19". As the load changes at time  $t= 4$  sec frequency is imbalanced and it goes below 50 but due to the controller operation at load side frequency again goes to desired value. It shows that the controller performs well to suppress the power fluctuations in the generation side. The change in frequency is within allowable limit as per the standards. The THD values of the

inverter output voltage is 4.5% it is within limits (5%) as per the standards of IEEE.

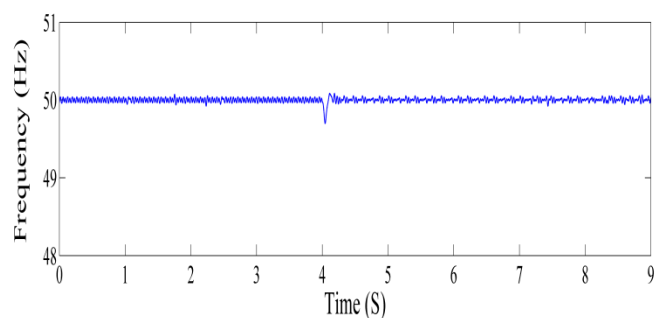


**Fig.19.** Load voltage Frequency (Hz)

## 5. Conclusion

In this paper, a fuzzy logic controller is implemented for power control in the HRES systems which works as per the power flow control strategies designed for the systems. Under different scenarios of power generation and power consumption by load the controller performs well and at the same time maintaining the battery SOC with in minimum and maximum limits. It avoids the battery degradation and increases its life. So it is economically benefited in long run of the system. It is analyzed from simulation results that power generation from PV, wind system always meet the load demand. The inverter controller supplies power for the load at desired reference voltage and frequency. The inverter controller is capable of supplying load at desired voltage and frequency.

## References

- [1] Zhang L, Li Y., "Optimal energy management of hybrid power system with two-scale dynamic programming", Power Systems Conference Exposition (PSCE), 2011 IEEE/PES, pp.1-8, March 2011.
- [2] Biswas I, Dash V, Bajpai P., "Sizing optimization of PV-FC-battery system with hybrid PSO-EO algorithm", IEEE Annual India Conference (INDICON), pp. 869-874, Dec 2012.
- [3] Behzadi MS, Niasati M., "Comparative performance analysis of a hybrid PV/FC/battery stand-alone system using different power management strategies and sizing approaches", International Journal of Hydrogen Energy, Vol.40, No.1, pp. 538-548, 2015.
- [4] Randa Kallel, Ghada Boukettaya, Lotfi Krichen, "Control Management Strategy of Stand-Alone Hybrid Power Micro-System using Super-Capacitor", International journal of Renewable Energy Research, Vol.4, No.1, pp. 210-213, 2014.
- [5] Kohsris, Plang klang B., "Energy management and control system for smart renewable energy remote power generation", Energy procedia ,Vol.9, pp.198-206, 2011.
- [6] Bouthaina Madaci, Rachid Chenni, Erol Kurt, Kamel Eddine Hemsas, "Design and control of a stand-alone hybrid power system", International Journal of Hydrogen Energy, Vol.41, Issue. 29, pp.12485-2496, 2016
- [7] Mirazimi SJ, Fathi M., "Analysis of hybrid wind/fuel cell/battery/diesel energy system under alaska condition", International Conference on Electrical Engineering/Electronics, Computer, Telecommunications and Information Technology (ECTI-CON), pp. 917-920, May 2011.
- [8] Jayalakshmi N.S., D.N.Gaonkar, Pramod Bhat Nempu, "Power Control of PV/Fuel Cell/Super capacitor Hybrid System for Stand-Alone Applications", International Journal of Renewable Energy Research, Vol.6, No.2, pp. 672-679, 2016.
- [9] S.G. Malla, C.N. Bhende, "Voltage control of stand-alone wind and solar energy system", Electrical Power and Energy Systems, Vol. 56, pp. 361-373, 2014.
- [10] T.Vigneysh, N.Kumarappan, "Autonomous operation and control of photovoltaic/solid oxide fuel cell/battery energy storage based micro grid using fuzzy logic controller", International Journal of Hydrogen Energy, Vol. 41, No. 3, pp. 1877-1891, 2015.
- [11] Zeng Qingrong, Chang Liuchen, "An advanced SVPWM-based predictive current controller for three-phase inverters in distributed generation systems", IEEE Transactions on Industrial Electronics, Vol. 55, No. 3, pp.1235-1246, 2008.
- [12] Chen Zhiyong, Luo An, Wang Huajun, Chen Yandong, Li Mingshen, Huang Yuan., "Adaptive sliding-mode voltage control for inverter operating in islanded mode in micro grid", International Journal of Electrical Power & Energy System, Vol.66, pp. 133-143, 2015.
- [13] Wang Fu-Cheng, Kuo Po-Chen, Chen Hsueh-Ju., "Control design and power management of a stationary PEMFC hybrid power system", International Journal of Hydrogen Energy, Vol. 38, No.14, pp. 5845-5856, 2013.
- [14] Hassan MA, Abido MA., "Optimal design of micro grids in autonomous and grid-connected modes using particle swarm optimization", IEEE Transaction on Power Electronics, Vol. 26, No. 3, pp. 755-769, 2011.
- [15] Al-Saedi Waleed, Lachowicz Stefan W, Habibi Daryoush, Bass Octavian, "Power flow control in grid-connected micro grid operation using particle swarm optimization under variable load conditions", International Journal of Electrical Power & Energy Systems, Vol.49, pp.76-85, 2013.
- [16] Wu Xiao-Juan, Huang Qi, Zhu Xin-Jian, "Power decoupling control of a solid oxide fuel cell and micro gas turbine hybrid power system", Journal of Power Sources, Vol. 196, No. 3, pp. 1295-1302, 2011.

- [17] Ahmad Shameem, Albatsh Fadi M, Mekhilef Saad, Mokhlis Hazlie, "Fuzzy based controller for dynamic Unified Power Flow Controller to enhance power transfer capability", *Energy Conversion Management*, Vol.79, pp.652-665, 2014.
- [18] Hiroshi N, Tatsuya N, Hiroshi M, Takenobu K., "Development of 100-W high-efficiency MPPT power conditioner and evaluation of TEG system with battery load", *Journal of Electronic Material*, Vol. 40, No.5, pp. 657-661, 2011.
- [19] Valenciaga F, Evangelista CA, "Control design for an autonomous wind based hydrogen production system", *International Journal of Hydrogen Energy*, Vol.35, Issue 11, pp. 5799-5807, 2010.
- [20] Dahmane M, Bosche J, El-Hajjaji A, Dafarivar M., "Renewable energy management algorithm for stand-alone system", *International Conference on Renewable Energy Research and Applications*, Madrid, Spain, pp. 621-26, October 2013.
- [21] Ribeiro E, Marques Cardoso AJ, Boccaletti C., "Standalone diesel photovoltaic system with batteries and super capacitors as energy storage components for telecommunications", *IEEE 34th International Telecommunications Energy Conference*, Arizona, USA, 30 Sep-4 Oct 2012.
- [22] Mohammad RM, Mohd FR, Ali AG, Mohd WM., "Control techniques for three-phase four-leg voltage source inverters in autonomous micro grids: a review", *Renewable Sustainable Energy Reviews*, Vol. 54, pp.1592-610, 2016.
- [23] C. N. Bhende, S. Mishra, Siva Ganesh Malla, "Permanent Magnet Synchronous Generator-Based Standalone Wind Energy Supply System", *IEEE Transaction on Sustainable Energy*, Vol. 2, No. 4, pp. 361-373, 2011.
- [24] Dahono, Agus Purwadi, Qamaruzzaman Pekik, "An LC Filter Design Method for Single-phase PWM Inverters", *Proceeding of 1995 International Conference on Power Electronics and Drive systems*, pp. 571-576, 1995.